

# Introduction to a motion control algorithm for the autonomous 4-wheel steering vehicle

Yongseong Cho, Kangmin Noh, Eunchan Lee and Hyunhwan Jeong\*

**Abstract**—This paper introduces a motion control algorithm for an autonomous four-wheel steering(4WS) vehicle system, which independently controls the steering angles of the front and rear wheels. This capability allows for three distinct driving modes: front steering mode, crab steering mode, and symmetrical steering mode. The proposed algorithm effectively uses these modes to achieve precise maneuverability, facilitating accurate navigation toward the target location. We conducted a kinematic analysis of the four-wheel steering vehicle, with a focus on its motion characteristics. A simple motion control law is developed using the kinematic analysis and the steering mode transition of the 4WS vehicle. To validate the feasibility and effectiveness of the proposed algorithm, initial numerical simulation results are presented.

## I. INTRODUCTION

Over the past decade, numerous studies on autonomous vehicles and mobile robots have been conducted, with many focusing on autonomous driving technology and Simultaneous Localization and Mapping (SLAM). Vehicle kinematic and dynamic analysis, along with the development of control algorithms, are integral components of research in the fields of autonomous vehicles and mobile robotics.

Raj, Ravi, and Andrzej Kos [1] present a thorough review of the development and applications of autonomous mobile robots, highlighting their growing influence on industries such as logistics, healthcare, and agriculture. Alatise and Hancke [2] address the key challenges encountered by autonomous mobile robots, with a particular focus on sensor fusion methods that improve navigation, obstacle avoidance, and environmental perception. Their analysis provided a critical evaluation of the strengths and weaknesses of various sensor fusion techniques. Taheri and Xia [3] present an in-depth review of the evolution of SLAM technology, emphasizing how advanced sensor fusion methods and machine learning have markedly improved the accuracy and robustness of SLAM systems in dynamic environments. Sanchez-Ibanez et al. [4] review a range of algorithms and techniques for path planning in autonomous mobile robots (AMRs), evaluating the strengths and limitations of classical, sample-based, and optimization-based approaches, with a particular emphasis on dynamic environments. Filipenko and Afanasyev [5] assess the performance of various algorithms

for indoor environments, using a prototype four-wheel steering mobile robot in their evaluations.

In the research field of 4WS vehicles, numerous studies have conducted kinematic and dynamic analyses, leading to the development of various control techniques.[6] [7] [8] [9] Tourajizadeh et al. [10] introduced an optimal control technique using a Linear Quadratic Regulator (LQR) and compared its performance with that of traditional two-wheel steering systems. He Bo [11] presented a 4WS mobile robot equipped with RTK-GPS, along with an estimator composed of an EKF (Extended Kalman Filter) and Runge-Kutta-based dead reckoning for precise navigation. Zhang et al. [12] introduced a fuzzy control and pure tracking model algorithm that improves path tracking accuracy and stability in 4WS agricultural vehicles. Lee and Li [13] presented kinematic and dynamic models for a mobile robot with four wheel steering and driving (4WIS4WID), along with a dynamic trajectory tracking control method. Tu et al. [14] focused on robust navigation control for a 4WIS agricultural robotic vehicle, demonstrating the effectiveness of advanced control strategies in enhancing stability and precision in challenging agricultural environments. Furthermore, novel steering mechanisms, including parallel maneuver, zero side slip maneuver [15], and symmetric steering systems [16], have been proposed to optimize the turning radius based on kinematic analysis.

Bae and Lee [17] developed a 4WS robot platform equipped with an adaptive control system designed for manual operation. This system enhances maneuverability and stability in complex environments by dynamically adjusting the steering in real-time based on user inputs. Similarly, Tan, Liu, and Xiong [18] implemented an MPC-based optimal control method that significantly improves path tracking accuracy in 4WS vehicles. Their research showed that the asymmetrical steering model excels in maneuverability within tight spaces, while the symmetrical steering model provides greater stability at high speeds, thereby validating the algorithm's effectiveness across various driving conditions.

As mentioned above, the 4WS vehicle mechanism has many kinematic advantages as in previous studies. In this paper, we propose a simple and efficient motion control algorithm based on these advantages of the 4WS vehicle. The steering mode transition strategy is implemented in the proposed control algorithm. The rest of the paper is organized as follows: Section II describes the kinematic analysis of the motion of the autonomous vehicle. In Section III, the derivation of the control law based on the kinematic analysis is explained. The initial experiments and their results are

Department of Control and Instrumentation Engineering, Korea University, 2522 Sejong-ro, Sejong city, Korea  
\*hyunhwanjeong@korea.ac.kr

This results was supported by "Basic Science Research Program(NRF-2022R111A3066094)", "Regional Innovation Strategy (2021RIS-004)" and "Industrial Strategic Technology Development Program (00443339)" funded by the Ministry of Education(MOE) and the Ministry of Trade, Industry & Energy(MOTIE, Korea)

addressed in Section IV. Conclusion and future works are located in Section V.

## II. VEHICLE MODELING

In this section, the kinematic model of the four-wheel steering vehicle is analyzed as a foundation for developing a new control algorithm. We used the 4WS which is replaced with equivalent single-track model to simplify the calculation, as shown in Fig. 1.

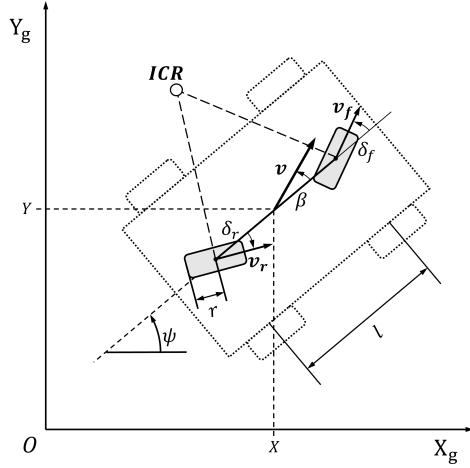


Fig. 1: 4WS Kinematic model

### A. Forward Kinematics

The vehicle's pose can be estimated utilizing its forward kinematic model. In this section, the forward kinematic model is depicted using the four-wheel steering model, as illustrated in Fig. 1. The position and velocity of the vehicle can be derived from its odometer data [10]. The side-slip angle,  $\beta$ , is

$$\beta = \tan^{-1} \frac{\tan \delta_f + \tan \delta_r}{2} \quad (1)$$

Where,  $\delta_f$  and  $\delta_r$  are the front and rear steering angles, respectively. The linear velocity ( $v$ ) and angular velocity ( $\omega$ ) of the vehicle can be computed from the front ( $\delta_f$ ) and rear ( $\delta_r$ ) wheel velocities using the following equations.

$$v = \frac{v_f \cos \delta_f + v_r \cos \delta_r}{2 \cos \beta} \quad (2)$$

$$\omega = \frac{v_f \sin \delta_f - v_r \sin \delta_r}{l} \quad (3)$$

Where  $r$  and  $l$  are the radius of wheel and the length of the wheelbase. Additionally, the velocities at the vehicle's center of mass can be obtained using the following equations.

$$\dot{x} = v \cos(\psi + \beta) \quad (4)$$

$$\dot{y} = v \sin(\psi + \beta) \quad (5)$$

$$\dot{\psi} = \frac{v \cos \beta (\tan \delta_f - \tan \delta_r)}{l} \quad (6)$$

Where,  $\psi$  denotes the angle of the chassis relative to the global coordinate frame.

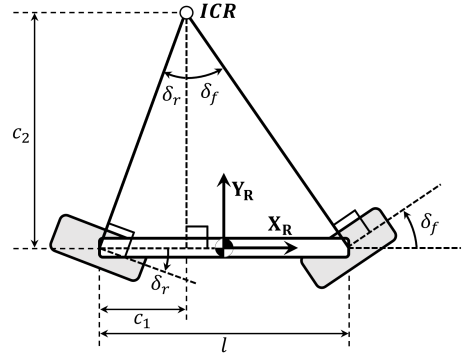


Fig. 2: 4WS steering model with ICR

### B. Inverse Kinematics

Contrary to forward kinematics, the wheel speeds and steering angles required to achieve the desired velocity and angular velocity can be determined using inverse kinematics. The four-wheel steering vehicle needs to satisfy the Ackermann geometry. Fig. 2 show the schematic configuration of the four-wheel steering vehicle. As shown in this figure, the front and rear steering angles are derived from the Instantaneous Center of Rotation (ICR), and vice versa [15]. From the position information of the ICR of the vehicle ( $C_1$  and  $C_2$  in the Fig. 2), the front and rear steering angle can be obtained as following equations.

$$\delta_f = \tan^{-1} \left( \frac{l - c_1}{c_2} \right) \quad (7)$$

$$\delta_r = \tan^{-1} \left( \frac{c_1}{c_2} \right) \quad (8)$$

Additionally, the vehicle's velocities for the front and rear wheels can be determined using Eqn. 2 and 3.

$$v_f = \frac{4v \cos \beta \sin \delta_r + l\omega \cos \delta_r}{2 \sin(\delta_f + \delta_r)} \quad (9)$$

$$v_r = \frac{4v \cos \beta \sin \delta_f - l\omega \cos \delta_f}{2 \sin(\delta_f + \delta_r)} \quad (10)$$

## III. CONTROL LAW

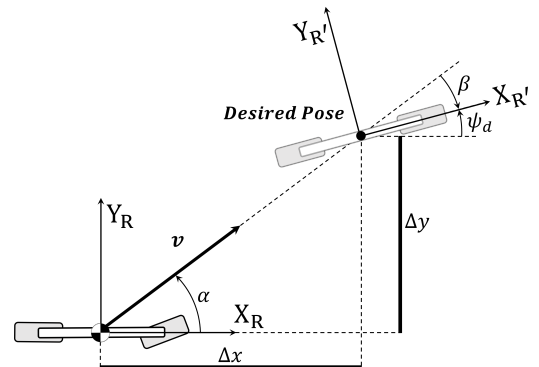


Fig. 3: Control scheme

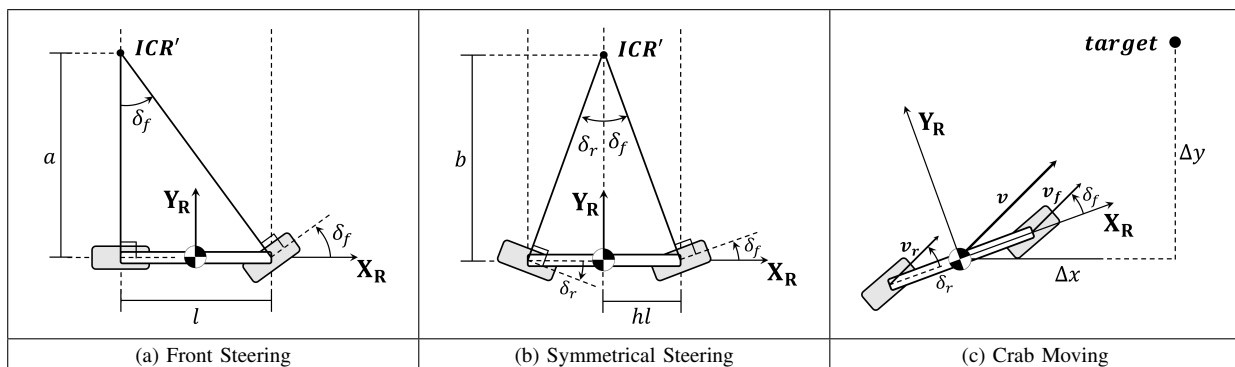


Fig. 4: Illustration of steering modes

In this section, we present the proposed control method for the four-wheel steering vehicle based on the kinematic model in the previous section. Fig. 3 illustrates the schematic diagram of the proposed vehicle control law. As depicted in the figure, the control law is formulated based on the distance and the orientation errors between the current pose  $X_c$  and the desired pose  $X_d$  of the vehicle. This approach is fundamentally similar to the previously established principles of the error tracking method for mobile robots [19], with the exception that the proposed method is applied within the local coordinate system. The error between the current pose and the desired pose can be defined as follows.

$$\rho = \sqrt{\Delta x^2 + \Delta y^2} \quad (11)$$

$$\alpha = \tan^{-1} \left( \frac{\Delta y}{\Delta x} \right) \quad (12)$$

$$\beta = \psi_d - \alpha \quad (13)$$

Here,  $\rho$  represents the distance from the current position to the desired position, while  $\alpha$  denotes the angular difference between the current and desired positions with respect to the local frame.  $\beta$  denotes the angle difference between target orientation angle  $\psi_d$  angle and heading angle. The desired linear and angular velocities can be generated from the defined errors ( $\rho$ ,  $\alpha$  and  $\beta$ ) and the proportional gains, as described in the following equations.

$$v = K_\rho \rho \quad (14)$$

$$\omega = K_\alpha \alpha + K_\beta \beta \quad (15)$$

The driving modes of the four-wheel steering vehicle can be defined as three distinct operation modes: front steering, symmetrical steering, and crab movement, as depicted in Fig. 4. Fig. 4 (a) shows the conventional front steering method commonly employed in standard vehicles. In this case, the vehicle controls its orientation using only the front wheels, with the ICR aligned along the rotational axis of the rear wheels. In the symmetrical steering mode, the steering angles of the front and rear wheels are rotated by the same angle but in opposite directions as shown in Fig. 4 (b). In this case, the ICR is located on the line perpendicular to the chassis, passing through the center of the vehicle.[16] In crab mode,

the front and rear wheels rotate at the same angle and in the same direction, producing linear movement of the vehicle without any rotation of the chassis (see Fig. 4 (c)).[15] A

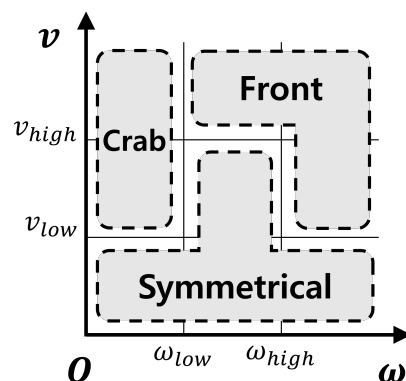


Fig. 5: Control law for steering mode transition

control law for transitioning between the vehicle's steering modes, as illustrated in Fig. 5, can be applied based on the required magnitudes of linear and angular velocities needed to reach the target position.

The driving speed and angular velocity of a vehicle equipped with a steering system can be defined using the Instantaneous Center of Rotation (ICR). Additionally, the ICR can be calculated differently depending on the mode, specifically the front-wheel steering mode and the symmetric steering mode, as presented in this paper. Fig. 6 shows the ICR for the desired linear and angular velocity of the vehicle in Eqn. 14 and 15. As show in the figure, desired velocities are defined on the center of mass of the vehicle.

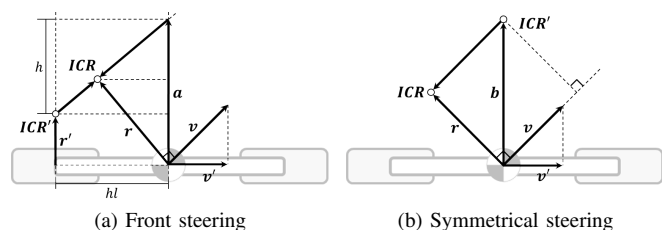


Fig. 6: Adjusting ICR for each steering modes

In the front steering mode, the ICR must be adjusted to align with the rotational axis of the rear wheels, as it is necessary for the ICR to be positioned on this line as shown in Fig. 6 (a). Additionally, because this paper assumes that the magnitudes of the front and rear steering angles are identical, the ICR in the symmetrical steering mode must be positioned on a line perpendicular to the vehicle's center of mass, as illustrated in Fig. 6 (b). In both figures, ICR' and ICR represent the adjusted and original positions of the ICR, respectively. The original ICR is calculated based on the desired velocities. From the relationship between linear velocity and angular velocity, expressed as  $\mathbf{w} \times \mathbf{r} = \mathbf{v}$ , the vector  $\mathbf{r}$  can be determined. In case of front steering mode, using the  $\mathbf{a} = (0, a_y)$  and  $\mathbf{r} = (r_x, r_y)$ , the adjusted ICR can be determined as follows:

$$\text{ICR}' = \left( -hl, a_y - \frac{hl(|a_y| - |r_y|)}{hl - |r_x|} \right) \quad (16)$$

In the symmetrical steering mode, the adjusted ICR can be represented by the following equation:

$$\text{ICR}' = \left( 0, \frac{r_x^2 + r_y^2}{r_y} \right). \quad (17)$$

In the crab mode, ICR adjustment is not necessary because this mode generates only linear velocity for the vehicle.

Using the adjusted ICR, the steering wheel angles and wheel velocities of the vehicle can be determined for each steering mode, as shown in table I. The steering angles of the front and rear wheels are determined according to the control law governing the proposed steering mode transitions, as illustrated in Figures 4 and 5.

TABLE I: Steering angles by steering modes

| Front                              | Symmetrical                          | Crab  |
|------------------------------------|--------------------------------------|---|
| $\delta_f = \tan^{-1} \frac{l}{a}$ | $\delta_f = \tan^{-1} \frac{hl}{b}$  | $\delta_f = \tan^{-1} \frac{\Delta y}{\Delta x} - \psi_c$ |
| $\delta_r = 0$                     | $\delta_r = -\tan^{-1} \frac{hl}{b}$ | $\delta_r = \tan^{-1} \frac{\Delta y}{\Delta x} - \psi_c$ |

#### IV. SIMULATION RESULT

To verify the validity of the proposed approach, we conduct a point tracking simulation. In this simulation, the target points are assigned in all four quadrants. In this simulation,

TABLE II: Simulation conditions

| test quadrant | $\psi_i$ [rad] | $\psi_d$ [rad] | $X_d$ [m]  |
|---------------|----------------|----------------|------------|
| 1/4           | 0              | 1.5708         | [10, 10]   |
| 2/4           | 0.6981         | 0.6109         | [-10, 8]   |
| 3/4           | 3.1416         | 3.1416         | [-10, -10] |
| 4/4           | 0.6981         | 1.3090         | [10, -10]  |

the steering angle and the velocity of the driving wheel are limited to  $40^\circ$  and 10 m/s, respectively. The initial position of the vehicle is  $[0, 0]$  for all simulations. The initial orientations and target poses of the simulations are given in Table II.

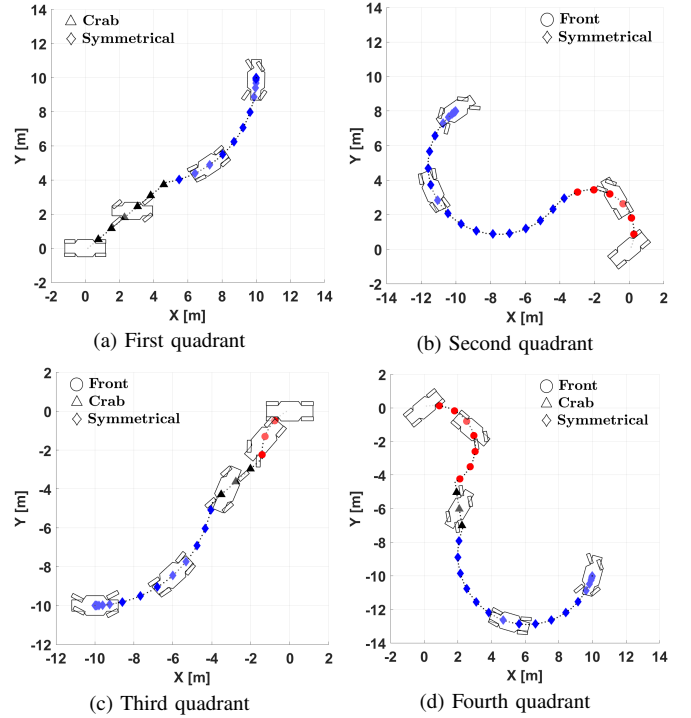


Fig. 7: Representative trajectories spanning all quadrants

Fig. 7 presents the results of the point tracking simulations. As shown in the figure, the vehicle equipped with the four-wheel steering motion controller proposed in this paper successfully reached the target positions and orientations in all quadrants. The figures illustrate the vehicle's trajectory from the initial pose to the desired pose. In each result, the trace corresponding to the crab steering mode is marked with triangles, the symmetrical steering mode is indicated by diamonds, and the front steering mode is represented by circles. The final tracking errors for the four different desired poses in the quadrant are presented in Table III. As indicated by the results, all tracking error values are on the order of less than  $10^{-4}$ .

TABLE III: Steady-state errors

| quadrant | $e_x$ [m]              | $e_y$ [m]              | $e_\psi$ [rad]         |
|----------|------------------------|------------------------|------------------------|
| 1/4      | $9.33 \times 10^{-8}$  | $8.97 \times 10^{-4}$  | $1.63 \times 10^{-4}$  |
| 2/4      | $2.09 \times 10^{-4}$  | $1.46 \times 10^{-4}$  | $-1.45 \times 10^{-4}$ |
| 3/4      | $-5.86 \times 10^{-4}$ | $-4.50 \times 10^{-8}$ | $2.62 \times 10^{-4}$  |
| 4/4      | $7.02 \times 10^{-5}$  | $2.62 \times 10^{-4}$  | $1.49 \times 10^{-4}$  |

Fig. 8 presents the simulation results, including tracking errors, vehicle velocities, and steering angles, for the simulation in the fourth quadrant. Fig. 8 shows the results of a motion control simulation for a target position in the second quadrant within the vehicle's coordinate system. As shown in Fig. 8 (a) and (b), the position error and the orientation error finally converge to zero. The result graphs in Fig. 8 (c) and (d) illustrate the variations in vehicle speed and angular velocity corresponding to changes in each steering mode. In the figures, the sections labeled (1), (2), and (3) correspond to the front steering, symmetric steering, and crab steering

mode, respectively. The changes in the steering angles of the front and rear wheels are illustrated in Fig. 8 (c). In this figure, the steering angles begin to oscillate after 2300 ms to adjust the orientation around the desired position.

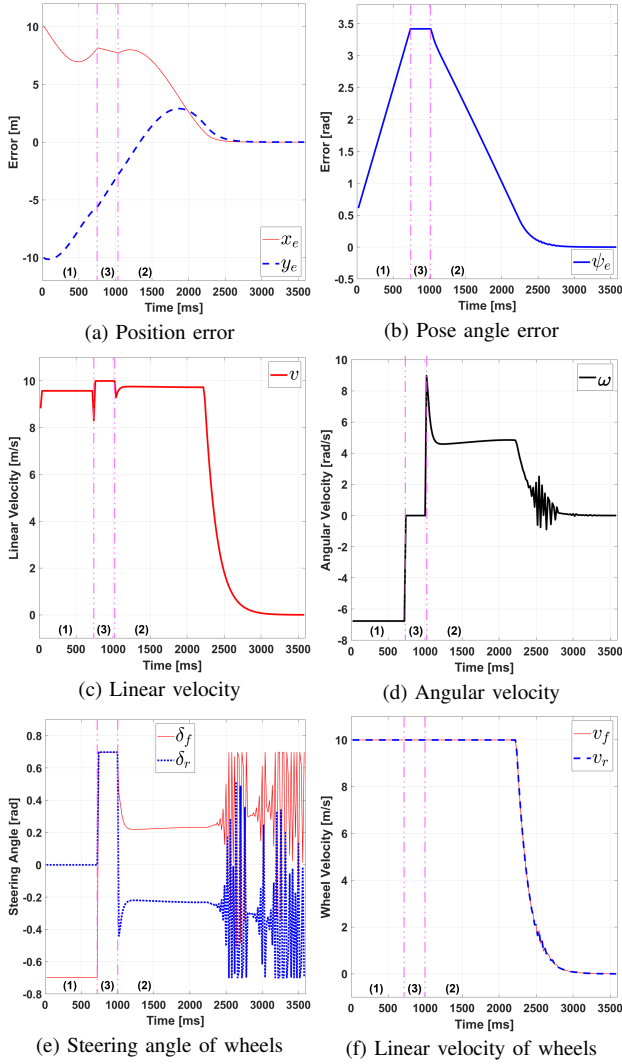


Fig. 8: Simulations results for the fourth quadrant case

## V. CONCLUSIONS & FUTURE WORKS

In this paper, we propose a motion control algorithm that takes into account the driving characteristics of a four-wheel steering vehicle. The proposed algorithm distinguishes between different driving modes of the four-wheel steering vehicle, which allows for both front and rear-wheel steering. It is designed to enable the vehicle to reach a designated destination by implementing specific control law tailored to each driving mode. We conducted initial simulations to demonstrate the feasibility and value of the proposed four-wheel steering motion control algorithm. In the future, we plan to enhance the proposed algorithm by incorporating independent control of the front and rear steering wheels. Additionally, we will consider the steering wheel velocity.

Finally, the refined algorithm will be implemented and tested on actual vehicle hardware.

## REFERENCES

- [1] Ravi Raj and Andrzej Kos. A comprehensive study of mobile robot: history, developments, applications, and future research perspectives. *Applied Sciences*, 12(14):6951, 2022.
- [2] Mary B Alatise and Gerhard P Hancke. A review on challenges of autonomous mobile robot and sensor fusion methods. *IEEE Access*, 8:39830–39846, 2020.
- [3] Hamid Taheri and Zhao Chun Xia. Slam; definition and evolution. *Engineering Applications of Artificial Intelligence*, 97:104032, 2021.
- [4] Jose Ricardo Sanchez-Ibanez, Carlos J Pérez-del Pulgar, and Alfonso García-Cerezo. Path planning for autonomous mobile robots: A review. *Sensors*, 21(23):7898, 2021.
- [5] Maksim Filipenko and Ilya Afanasyev. Comparison of various slam systems for mobile robot in an indoor environment. In *2018 International Conference on Intelligent Systems (IS)*, pages 400–407. IEEE, 2018.
- [6] KN Spentzas, Ibrahim Alkhalizi, and Miroslav Demic. Kinematics of four-wheel-steering vehicles. *Forschung im Ingenieurwesen*, 66(5):211–216, 2001.
- [7] Calequela JT Manuel, Max MD Santos, and Angelo M Tusset. Mathematical modeling attributed to kinematics and dynamics of a vehicle with 4-wheels. *The European Physical Journal Special Topics*, 230(18):3663–3672, 2021.
- [8] Robert Grepl, Josef Vejlupek, Vojtech Lambersky, Michal Jasansky, Filip Vadlejch, and Pavel Coupek. Development of 4ws/4wd experimental vehicle: platform for research and education in mechatronics. In *2011 IEEE International Conference on Mechatronics*, pages 893–898. IEEE, 2011.
- [9] Huipeng Chen, Sen Chen, Rougang Zhou, Xiaoyan Huang, and Shaopeng Zhu. Research on four-wheel independent steering intelligent control strategy based on minimum load. *Concurrency and Computation: Practice and Experience*, 33(9):e6145, 2021.
- [10] Hami Tourajzadeh, Mohsen Sarvari, and Sadegh Ordoo. Modeling and optimal control of 4 wheel steering vehicle using lqr and its comparison with 2 wheel steering vehicle. In *2018 6th RSI International Conference on Robotics and Mechatronics (IcRoM)*, pages 106–113. IEEE, 2018.
- [11] He Bo. Precise navigation for a 4ws mobile robot. *Journal of Zhejiang University-SCIENCE A (Applied Physics & Engineering)*, 7(2):185, 2006.
- [12] Chengliang Zhang, Guanlei Gao, Chunzhao Zhao, Lei Li, Changpu Li, and Xiyuan Chen. Research on 4ws agricultural machine path tracking algorithm based on fuzzy control pure tracking model. *Machines*, 10(7):597, 2022.
- [13] Ming-Han Lee and Tzuu-Hseng S. Li. Kinematics, dynamics and control design of 4wis4wid mobile robots. *The Journal of Engineering*, 2015(1):6–16, 2015.
- [14] Xuyong Tu, Jingyao Gai, and Lie Tang. Robust navigation control of a 4wd/4ws agricultural robotic vehicle. *Computers and Electronics in Agriculture*, 164:104892, 2019.
- [15] Yuhanes Dedy Setiawan, Trong Hai Nguyen, Pandu Sandi Pratama, Hak Kyeong Kim, and Sang Bong Kim. Path tracking controller design of four wheel independent steering automatic guided vehicle. *International Journal of Control, Automation and Systems*, 14:1550–1560, 2016.
- [16] V Arvind. Optimizing the turning radius of a vehicle using symmetric four wheel steering system. *International Journal of Scientific & Engineering Research*, 4(12):2177–2184, 2013.
- [17] Beomsu Bae and Dong-Hyun Lee. Design of a four-wheel steering mobile robot platform and adaptive steering control for manual operation. *Electronics*, 12(16):3511, 2023.
- [18] Xiaojun Tan, Deliang Liu, and Huiyuan Xiong. Optimal control method of path tracking for four-wheel steering vehicles. In *Actuators*, volume 11, page 61. MDPI, 2022.
- [19] Roland Siegwart, Illah Reza Nourbakhsh, and Davide Scaramuzza. *Introduction to autonomous mobile robots*. MIT press, 2011.